EMPIRICAL MODE DECOMPOSITION BASED SOFT-THRESHOLDING

Yannis Kopsinis, and Stephen (Steve) McLaughlin

Institute for Digital Communications, School of Engineering and Electronics, the University of Edinburgh
Alexander Graham Bell Bldg, King's Buildings, EH9 3JL, Edinburgh, UK
email: {y.kopsinis,Steve.McLaughlin}@ed.ac.uk

ABSTRACT

Inspired by the wavelet soft thresholding principle, shrinkage methods suited for the thresholding of the decomposition modes resulting from applying EMD to a signal are developed in this paper. We show, that although a direct application of this principle is not feasible in the EMD case, it can be appropriately adapted by exploiting the special characteristics of the EMD decomposition modes. Moreover, the SCAD thresholding rule is also incorporated and an iterative soft thresholding procedure is proposed which leads to enhanced denoising performance.

1. INTRODUCTION

The Empirical mode decomposition (EMD) method [1], [2], [3] is an algorithm for the analysis of multicomponent signals [4] that breaks them down into a number, say L, of amplitude and frequency modulated (AM/FM) signals, $h^{(i)}(t),\ i = 1,2,\ldots,L$, termed intrinsic mode functions (IMFs). In contrast to conventional decomposition methods such as wavelets, which perform the analysis by projecting the signal under consideration onto a number of predefined basis vectors, EMD expresses the signal as an expansion of basis functions which are signal-dependent, and are estimated via an iterative procedure called sifting. By construction, the IMFs share the following properties: They are zero mean, all their maxima and minima are positive and negative respectively and they are narrowband signals allowing for the existence of both amplitude and frequency modulation (AM/FM). In other words, the $N(i)$ extrema of $h^{(i)}(t)$ positioned at time instances $\mathbf{r}^{(i)} = [r_1^{(i)},\ r_2^{(i)},\ldots,\ r_{N(i)}^{(i)}]$ and the corresponding IMF points $h^{(i)}(r_j^{(i)}),\ j = 1,\ \ldots,\ N(i)$ will alternate between maxima and minima, i.e., positive and negative values. As a result, in any pair of extrema, $\mathbf{r}_j^{(i)} = [h^{(i)}(r_j^{(i)}), h^{(i)}(r_{j+1}^{(i)})]$, corresponds a single zero-crossing $z_j^{(i)}$. Moreover, each IMF, say the one of order i, have fewer extrema than all the lower order IMFs, $j = 1,\ldots,\ i-1$, occupying lower frequencies locally in the time-frequency domain than preceding ones. Fig. 1 depicts, as an example the first, fifth, sixth and ninth IMF resulting from the EMD analysis of a well studied piece-wise regular signal [5] (Fig. 1a) corrupted by white Gaussian noise corresponding 5dB signal to noise power ratio (SNR).

One of the tasks in which EMD can prove to be useful is signal denoising. In this paper, inspired by wavelet soft-thresholding, novel EMD-based denoising techniques are developed and tested in different signal scenarios. It is also shown, that although the main principles between wavelet and EMD soft thresholding are the same, in the case of EMD, the thresholding operation has to be properly adapted in order to be consistent with the special characteristics of the signal modes resulting from EMD.

2. WAVELET SOFT-THRESHOLDING

Employing a chosen orthonormal wavelet basis, an orthogonal $N \times N$ matrix $\mathbf{W}$ is appropriately built [6] which in turn leads to the discrete wavelet transform (DWT)

$$\mathbf{c} = \mathbf{W}\mathbf{x}$$

where, $\mathbf{x} = [x(1),\ x(2),\ldots,\ x(N)]$ is the vector of the signal samples and $\mathbf{c} = [c_1,\ c_2,\ldots,\ c_N]$ contains the resultant wavelet coefficients. Under white Gaussian noise conditions and due to the orthogonality of matrix $\mathbf{W}$, any wavelet coefficient c_i follows normal distribution with variance the noise variance σ and mean the corresponding coefficient value $\bar{c}_i$ of the DWT of the noiseless signal $\bar{x}(t)$. Provided that the signal under consideration is sparse in the wavelet domain the DWT is expected to distribute the total energy of $\bar{x}(t)$ in only a few wavelet components lending themselves to high amplitudes. As a result, the amplitude of most of the wavelet components is attributed to noise only. The fundamental reasoning of wavelet soft thresholding is to set to zero all the components which are lower than a threshold related to noise level and appropriately shrink the rest of the components by an amount equal to the threshold. More specifically, the soft thresholding operator is defined by:

$$\rho_T(y) = \begin{cases} \text{sgn}(y)(|y| - T), & |y| > T \\ 0, & |y| \le T, \end{cases} \tag{1}$$

where, sgn indicates the sign function. Then, the estimated denoised signal is given by

$$\tilde{\mathbf{x}} = \mathbf{W}^T \tilde{\mathbf{c}} \tag{2}$$

where, $\tilde{\mathbf{c}} = [\rho_T(c_1),\ \rho_T(c_2),\ \ldots,\ \rho_T(c_N)]$ and $\mathbf{W}^T$ denotes transposition of matrix $\mathbf{W}$.

The conventional soft-thresholding rule shifts the estimator by an amount of T even when the wavelet components have energy well beyond the noise level creating unnecessary bias. Such an effect can be reduced by the smoothly clipped absolute deviation (SCAD) penalty [7] which is a more complex thresholding strategy

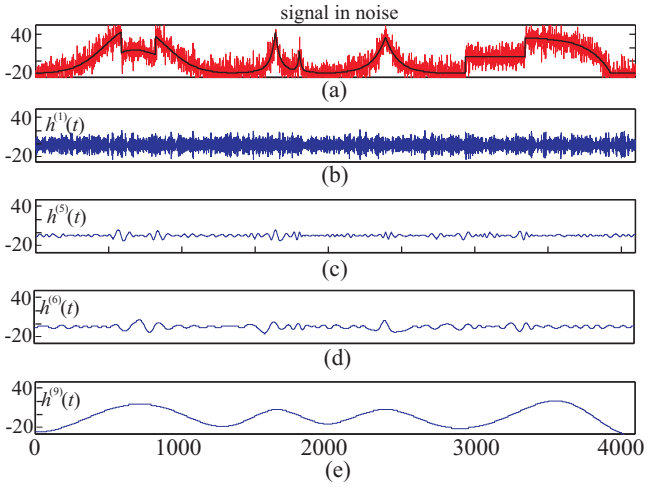

Figure 1: Empirical mode decomposition of the noisy signal shown in (a).

The insightful comments of the reviewers were extremely useful and are gratefully acknowledged.

in order not to penalize the wavelet components having large values. The SCAD threshold is given by:

$$\rho_T(y) = \begin{cases} \mathrm{sgn}(y)\max(0,|y|-T), & |y| \le 2T \\ \frac{(\alpha-1)y-\alpha T\mathrm{sgn}(y)}{\alpha-2}, & 2T < |y| \le \alpha T \\ y, & |y| > \alpha T, \end{cases} \quad (3)$$

where, α, based on Bayesian arguments, is recommended to set equal to 3.7. Apart from the soft thresholding methods described above, their translation invariant [5] versions are of interest and they will be studied in the simulation section.

3. EMPIRICAL MODE DECOMPOSITION BASED SOFT-THRESHOLDING

EMD performs a subband like filtering resulting in essentially uncorrelated IMFs [8], [9]. Although the equivalent filter-bank structure is by no means pre-determined and fixed as in wavelet decomposition, one can in principle perform thresholding in each IMF in order to locally exclude low energy IMF parts which are expected to be significantly corrupted by noise. Some preliminary results have already appeared very recently in [10], [11], [12] where the wavelet thresholding idea is directly applied to the EMD case. For example, in the case of standard soft thresholding, a direct application in the EMD case translates to:

$$\tilde{h}^{(i)}(t) = \begin{cases} \mathrm{sgn}(h^{(i)}(t))(|h^{(i)}(t)|-T_i), & |h^{(i)}(t)| > T_i \\ 0, & |h^{(i)}(t)| \le T_i, \end{cases} \quad (4)$$

where, $\tilde{h}^{(i)}(t)$ indicates the ith thresholded IMF. The reason for adopting different thresholds T_i per mode i will become clearer in the sequel.

A generalised reconstruction of the denoised signal is given by

$$\hat{x}(t) = \sum_{i=M_1}^{M_2} \tilde{h}^{(i)}(t) + \sum_{i=M_2+1}^{L} h^{(i)}(t) \quad (5)$$

where, the introduction of parameters M_1 and M_2 gives us flexibility on the exclusion of the noisy low order IMFs and on the optional thresholding of the high order ones which in white Gaussian noise conditions contain little noise energy.

As it has been discussed in [13] the direct application of hard thresholding to the decomposition modes is in principle wrong introducing significant discontinuities in the reconstructed signal. This is happening due to the fact that IMFs resemble an AM/FM modulated sinusoid with zero mean. As a result, it is guaranteed that, even in a noiseless case, in any interval $\mathbf{z}_j^{(i)} = [z_j^{(i)}\ z_{j+1}^{(i)}]$, the absolute amplitude of the ith IMF, $i = 1, 2, \ldots, N$, will drop below any non-zero threshold in the proximity of the zero-crossings $z_j^{(i)}$ and $z_{j+1}^{(i)}$. Similar arguments are valid in the case of soft thresholding. A solution to this drawback of direct thresholding is to infer for each one of the intervals $\mathbf{z}_j^{(i)}$ if they are noise-dominant or signal-dominant based on the single extrema $h^{(i)}(r_j^{(i)})$ that correspond to this interval. If the signal is absent, the absolute value of this extrema will lie below the threshold. Alternatively, in the presence of strong signal, the extrema value can be expected to exceed the threshold. Practically, the result of wavelet soft thresholding on, e.g. positive wavelet components that exceed the threshold is that the latter is shrinked by an amount equal to the threshold. With respect to soft thresholding all the IMF samples that corresponds to zero-crossing interval with extremum exceeding the threshold have to be reduced in a smooth way in order for the extremum to get reduced exactly by an amount equal to the threshold. Fig. 2 describes the similarities between wavelet and EMD soft thresholding. After wavelet soft thresholding (Fig. 2a), all the original components, shown with thick gray lines, which are larger in absolute value from the threshold, shown with green line, are shrinked by the value of the threshold T. The rest of the components are set to zero. In the case of EMD soft thresholding, the extrema of the thresholded IMF, which are the extrema having absolute value that exceed the threshold are lower by the value of T compared to the original ones. The values of the IMF points belonging to the zero-crossing interval of the thresholded extrema are linearly reduced as well. The rest of the IMF values are set to zero.

Mathematically, the described soft thresholding operation, hereafter referred to as EMD soft interval thresholding (EMD-SIT), yelds:

$$\tilde{h}^{(i)}(\mathbf{z}_j^{(i)}) = \begin{cases} h^{(i)}(\mathbf{z}_j^{(i)})\frac{|h^{(i)}(r_j^{(i)})|-T_i}{|h^{(i)}(r_j^{(i)})|}, & |h^{(i)}(r_j^{(i)})| > T_i \\ 0, & |h^{(i)}(r_j^{(i)})| \le T_i, \end{cases} \quad (6)$$

The thresholding rule above guaranties that when any extremum $|h^{(i)}(r_j^{(i)})|$ exceeding the threshold its thresholding lead to a shrink extremum expressing by $\tilde{h}^{(i)}(r_j^{(i)}) = \mathrm{sgn}(h^{(i)}(r_j^{(i)}))(|h^{(i)}(r_j^{(i)})| - T_i)$.

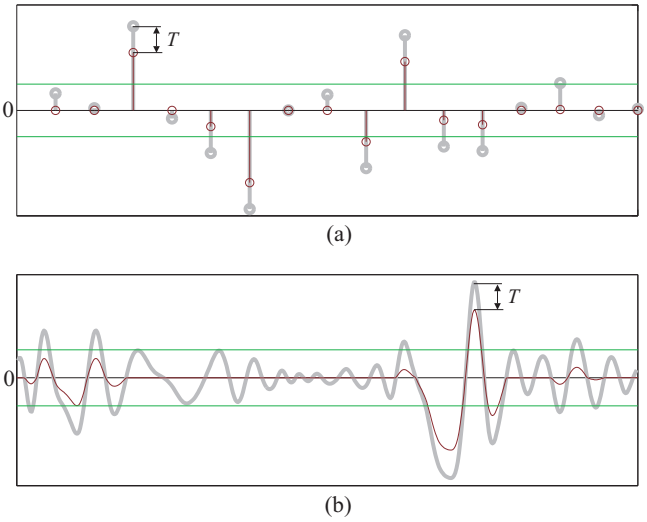

Figure 2: Wavelets (a) and EMD (b) soft thresholding. Thick gray lines indicate the wavelet components and the IMF before thresholding and dark thin lines shows the result of soft thresholding.

Similarly to (6), the SCAD rule of Eq. (3) in the case of EMD thresholding translates to:

$$\tilde{h}^{(i)}(\mathbf{z}_j^{(i)}) = \begin{cases} h^{(i)}(\mathbf{z}_j^{(i)})\frac{\max(0,|h^{(i)}(r_j^{(i)})|-T_i)}{|h^{(i)}(r_j^{(i)})|}, & |h^{(i)}(r_j^{(i)})| \le 2T_i \\ h^{(i)}(\mathbf{z}_j^{(i)})\frac{(\alpha-1)|h^{(i)}(r_j^{(i)})|-\alpha T_i}{(\alpha-2)|h^{(i)}(r_j^{(i)})|}, & 2T_i < |h^{(i)}(r_j^{(i)})| \le \alpha T_i \\ 1, & |h^{(i)}(r_j^{(i)})| > \alpha T_i, \end{cases} \quad (7)$$

With respect to the threshold selection, the universal threshold $T = \sigma\sqrt{2\ln N}$, with N being the signal length, is a popular candidate. In this study, multiples of the universal threshold, i.e., $C\sigma\sqrt{2\ln N}$ will be used, where C is a constant. The standard deviation of the noise, in the case of wavelet thresholding, is estimated using robust median-based estimation [5]. A somewhat different approach have to be followed for the estimation of the EMD-based denoising thresholds. In contrast to wavelet denoising where thresholding is applied to the wavelet components, in the EMD case, thresholding is applied to the N samples of each IMF which are basically the signal portion contained in each adaptive subband. An equivalent procedure in the wavelet method would be to perform thresholding on the reconstructed signals after performing the

synthesis function on each scale separately. As a consequence, the IMF samples are not Gaussian distributed with variance equal to the noise variance as the wavelet components are irrespective of scale. In fact, the noise contained in each IMF is coloured[1] *having different energy* in each mode. In that sense, EMD denoising is mostly related to wavelet denoising of signals corrupted by coloured noise where the thresholds have to be scale dependent. In our study of thresholds, multiples of the IMF dependent universal threshold, i.e., $T_i = C\sqrt{E_i 2\ln N}$, where E_i is the energy of the ith IMF that result from the EMD analysis of white Gaussian noise having variance the variance of noise which corrupts the signal under consideration are used. It has been shown [8] that $E_i,\ i = 2,3,\cdots,L$ can be estimated using equation

$$\hat{E}_i = \frac{E_1}{0.719} 2.01^{-i},\ i = 2,\ 3,\ 4,\ldots \tag{8}$$

where, E_1 is the variance of the first IMF. Note that the approximation (8) is slightly dependent on the number of sifting iterations as it has been stated in [8]. However, although it is apparently not optimal with respect to the number of sifting iterations used in the simulations section, it appeared to be accurate enough at least for the EMD configurations adopted in this paper.

Matlab scripts for implementing the EMD-based soft thresholding methods presented here can be found online at http://www.see.ed.ac.uk/∼ykopsini/emd/emd.html

4. ITERATIVE EMD INTERVAL-THRESHOLDING

Denoising performance can be improved by using the iterative scheme introduced in [13]. According to this, a number of denoised versions of the signal under consideration are obtained iteratively in order to enhance the tolerance against noise by averaging them. The different denoised versions of the noisy signal are constructed by decomposing different noisy versions of the signal under consideration itself. The answer on how, having a signal buried in noise, can we produce different noisy versions of the actual noise-free signal stems from within the EMD concept exploiting the characteristics of the first IMF. We know that in white Gaussian noise conditions, the first IMF is mainly noise, and more specifically comprises the larger amount of noise compared to the rest of the IMFs. By random circulating the samples of the first IMF and then adding the resulting noise signal to the sum of the rest of the IMFs we can obtain a different noisy-version of the original signal. In fact, in the case where the first IMF consists of noise only, then the total noise variance of the newly generated noisy-signal is the same as the original one. However, when the signal SNR is high, is likely to contain some signal portions as well. If this is the case, then by randomly circulating the samples of the first IMF, the information signal carried on it will spread out contaminating the rest of the signal along its length. In such an unfortunate situation, the denoising performance will decline. In order to bypass this disadvantage, in this paper we present a moderate modification of the scheme above. It is not the first IMF that is directly circulated but the first IMF after having all the parts of the useful information signal that it contains removed. The "extraction" of the information signal from the first IMF can be realized with any thresholding method, either EMD-based or wavelet-based. It is important to note that any useful signal resulting from the thresholding operation of the first IMF has to summed up with the partial reconstruction of the last $L-1$ IMFs.

The above EMD denoising technique, hereafter refered to as clear first IMF Iterative EMD soft interval-thresholding (EMD-SCIIT) is summarised in the following steps:

1. Perform an EMD expansion of the original noisy signal x.
2. Perform a thresholding operation to the first IMF of $x(t)$ to obtain a denoised version $\tilde{h}^{(1)}(t)$ of $h^{(1)}(t)$.
3. Compute the actual noise signal that existed in $h^{(1)}(t)$, $h_n^{(1)}(t)$=$h^{(1)}(t) - \tilde{h}^{(1)}(t)$
4. Perform a partial reconstruction using the last $L-1$ IMFs plus the information signal contained in the first IMF, $x_p(t) = \sum_{i=2}^{L} h^{(i)}(t) + \tilde{h}^{(1)}(t)$.
5. Randomly circulate the sample positions of the noise-only part of the first IMF, $h_a^{(1)}(t) = \text{CIRCULATE}(h_n^{(1)}(t))$.
6. Construct a different noisy version of the original signal, $x_a(t) = x_p(t) + h_a^{(1)}(t)$.
7. Perform EMD on the new noisy signal $x_a(t)$.
8. Perform the EMD-SIT denoising (Eq. 6 or 7) on the IMFs of $x_a(t)$ to obtain a denoised version $\tilde{x}_1(t)$ of x.
9. Iterate $K-1$ times between steps 5-8 , where K is the number of averaging iterations in order obtain K denoised versions of x, i.e., $\tilde{x}_1,\ \tilde{x}_2,\ldots,\tilde{x}_K$.
10. Average the resulted denoised signals $\tilde{x}(t) = \frac{1}{K}\sum_{k=1}^{K} \tilde{x}_k(t)$ in order to obtain the final denoised signal estimate.

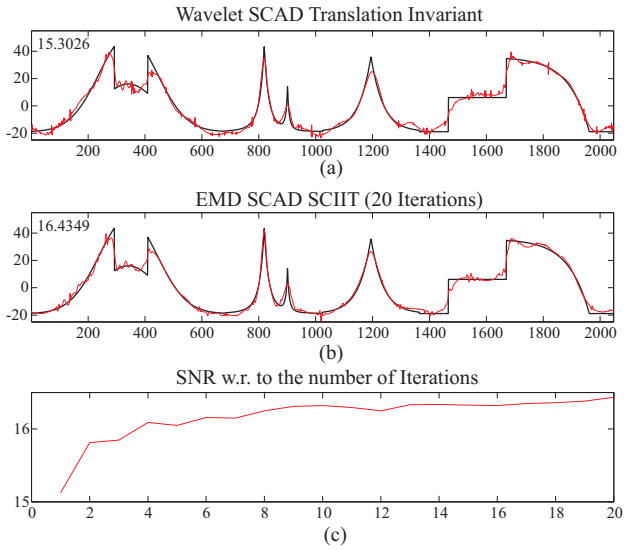

Figure 3: The result of the wavelet translation invariant with SCAD soft thresholding rule (a) and the EMD-SCIIT with SCAD thresholidng 20 iterations (b). (c) shows the achieved SNR w.r. to the number of iterations.

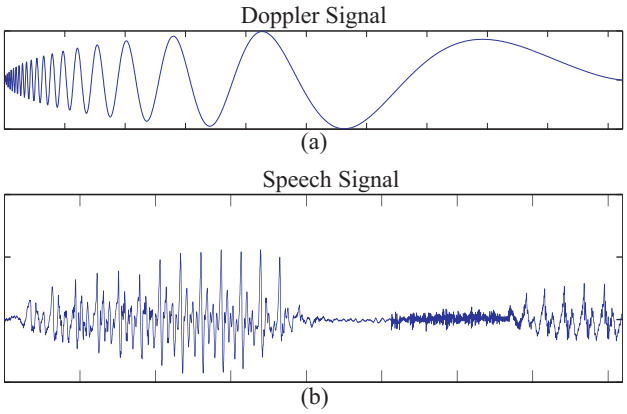

Figure 4: Some of the signals used for validation of the denoising methods.

Fig. 3a shows the denoising result when wavelet translation invariant with SCAD soft thresholding rule is applied on the

[1]There is strong evidence that at least in the noise-only case the distribution of the IMF samples is still Gaussian [9].

piecewise-regular signal. For comparison, the denoised signal that result from 20 iterations K, of EMD-SCIIT with SCAD thresholding. The SNRs achieved with the two methods are illustrated at the top left corner of the figures. The noisy signal used was that described in Fig. 1a. The proposed iterative procedure has enhanced the denoising capabilities of EMD as it can be seen in Fig. 3c where the increment in SNR of the denoised signal is plotted with respect to the number of iterations. In both Wavelet and EMD denoising the threshold value used was half the universal threshold since it has been considered an appropriate choice when soft thresholding is used [5]. However, in the simulations section, a broader range of threshold values will be examined.

5. SIMULATION RESULTS

Apart from the piecewise-regular signal, the Doppler test signal shown in Fig. 4a and a real speech signal segment (Fig. 4b) have been used for the validation of the proposed denoising techniques. Each of the artificial test signals is sampled and tested with four different sampling frequencies resulting in four versions per signal having 1024, 2048, 4096 and 8192 samples. The adopted wavelet filter is the symmlet of order 8 and the EMD is realised using 8 sifting iterations per IMF extraction. The adoption of a fixed number of sifting iterations might lead to modes which do not strictly comply with the IMF characteristics. More specifically, it is possible to find two or even more maxima (or minima) between neighboring zero-crossings. In such cases, the thresholding is naturally performed based on the largest (smallest) value of the maxima (minima) lying between consecutive zero-crossings. The results shown correspond to ensemble average of 50 independent noise generalizations. Moreover, the adopted performance measure is the SNR after denoising which corresponds to SNR values of 0, 5, 10 and 15 dB before denoising. To start with, a thorough denoising performance

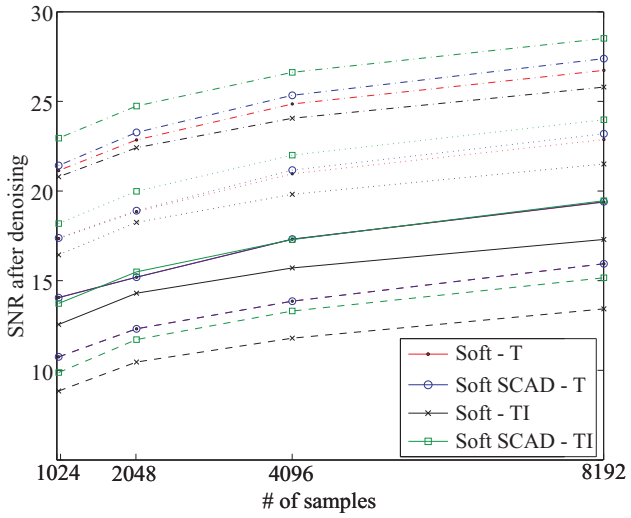

Figure 5: Denoising performance of different wavelet soft thresholding techniques.

evaluation of the developed and wavelet-based methods is realised using the piece-wise regular signal. Fig. 5 depicts the performance comparison between the standard (Soft-T) and translation invariant (Soft-TI) wavelet soft thresholding techniques including their SCAD versions. The performance curves correspond to SNR after denoising versus number of signal samples and they are grouped in 4 sets associated with 15dB SNR before denoising (dashed-dotted curves), 10dB SNR (dotted curves), 5dB SNR (solid curves) and 0dB SNR (dashed curves). We observe that the more robust performance is achieved with the translation invariant method when the SCAD thresholding rule is used which outperforms the rest of the methods especially when the noise is relatively low (15 dB). With respect to the newly developed EMD-based methods (Fig. 6) the soft EMD interval thresholding with (EMD SCAD-SIT) and without (EMD-SIT) the SCAD rule are examined together with their iterative counterparts (EMD SCAD-SCIIT and EMD-SCIIT) using 20 iterations. It can be seen that the iterative thresholding principle leads to enhanced performance irrespectively of the noise level and SCAD threshold is helpful when the signal SNR is 5dB and above. In all the simulations above and the ones that follows, the SNR

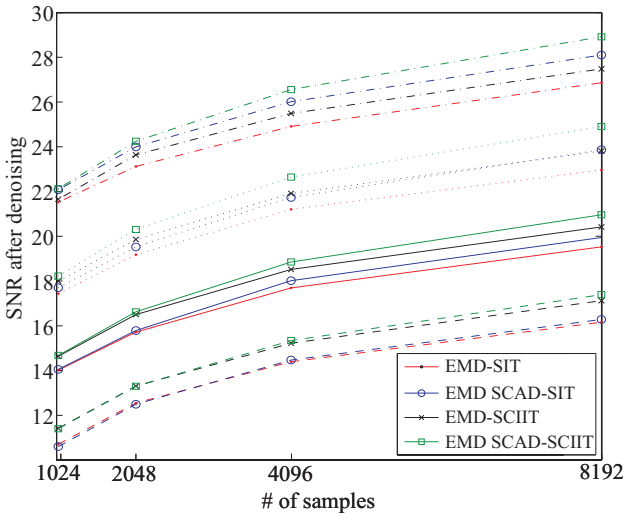

Figure 6: Denoising performance of different EMD soft thresholding techniques.

values shown correspond to optimized values for the several parameters that each method use such as the primary resolution level for the wavelet based denoising techniques and parameters M_1, M_2 of equation (5) for the EMD based denoising. The utility of parameter M_2 is similar to the primary resolution level in the case of wavelet thresholding, which indicates the level above which the wavelet components are thresholded. In the current study, an average choice of M_2 was 4. Moreover, it is worthy to note that when the SCAD principle is adopted, the choice of M_2 is less critical than when standard soft thresholding is used. With respect to M_1 is good to get reduced as the noise level decreases starting from 4 for 0dB SNR and going to 1 for 15 dB. Finally, the best among 9 threshold values was tested for each one of the different SNR/sampling

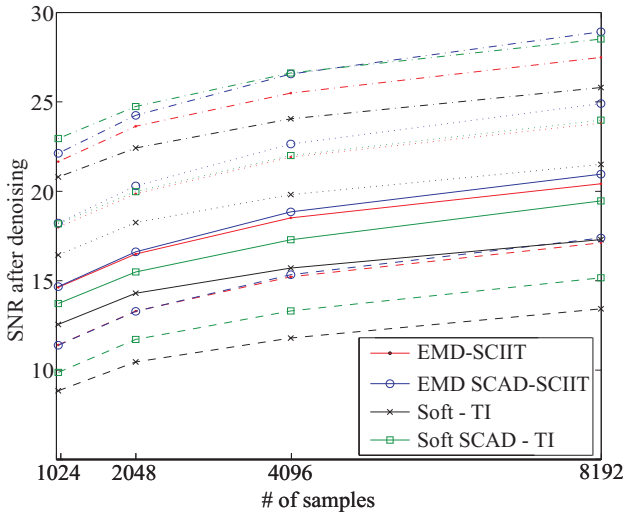

Figure 7: Performance of the piecewise-regular signal denoising.

frequency simulation setups. The 9 thresholds were calculated by multiplication of the universal threshold with the constants 0.2 up to 1 with steps of 0.1. It turned out that in the vast majority of simulation examples and all the different simulation setups, the best threshold for the EMD-based methods was found to be between 0.3 to 0.4 times the universal threshold with a small performance discrepancy for any threshold between the above values. The picture is similar in the case of wavelet thresholding with the difference that the optimum threshold values were 0.4 and 0.5 times the universal threshold when the translation invariant principle is used and 0.5 to 0.7 when the translation invariant principle was not used.

In Fig. 7, a comparison between the translation invariant wavelet and the iterative thresholding EMD techniques is depicted. We observe that EMD-based denoising using SCAD threshold outperforms the wavelet-based techniques especially when the noise is high. However, as long as the noise increases, Soft SCAD-TI reaches end even exceeds the EMD performance. This trend is similar to the one observed in the case of hard thresholding [13]. For

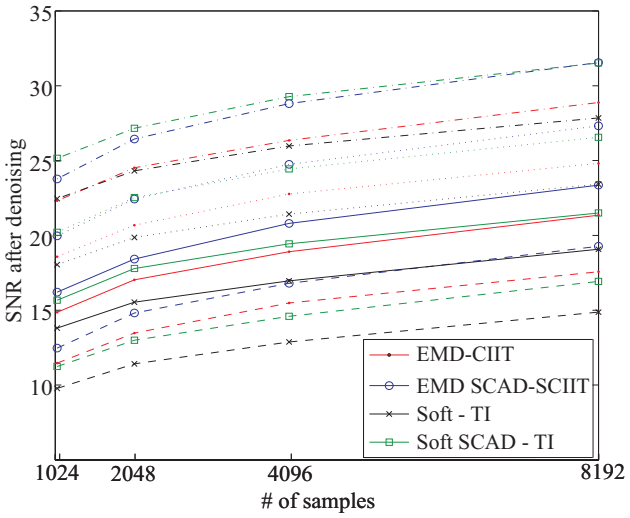

Figure 8: Performance of the Doppler signal denoising.

the case of the Doppler signal shown in Fig. 4(a), the performance results are illustrated in Fig. 8. Similar conclusions with the ones of the piecewise-regular signal can be drawn with the only difference that the achieved improvement when the SCAD threshold is used is more profound.

Methods	SNR			
	0 dB	5 dB	10 dB	15 dB
EMD-CIIT	9.99	13.32	16.63	20.25
EMD SCAD-CIIT	10.8	13.93	17.34	20.86
Soft-TI	8.55	12.06	15.58	19.44
Soft SCAD-TI	9.59	13.25	16.75	20.4

Table 1: SNR performance of EMD and wavelet-based denoising methods applied on a speech signal.

The SNR of the denoised speech signal of Fig. 4b and the corresponding variances of the SNR estimates over the 50 ensemble averages are shown in Tables 1 and 2 respectively. We observed that with this real signal the proposed denoising techniques performs with a similar to the test signals way. Moreover, the variance that the EMD denoising exhibits is slightly higher than that of the wavelet thresholding techniques. With respect to computational complexity, the EMD-based denoising is much more demanding than wavelet thresholding. However, although significant complexity reduction of EMD is feasible, low complexity EMD variants have not yet appeared in the literature.

Methods	Variance			
	0 dB	5 dB	10 dB	15 dB
EMD-CIIT	0.053	0.023	0.023	0.019
EMD SCAD-CIIT	0.038	0.027	0.021	0.019
Soft-TI	0.032	0.022	0.016	0.015
Soft SCAD-TI	0.031	0.021	0.014	0.016

Table 2: Variance of EMD and wavelet-based denoising methods when applied on a speech signal.

6. CONCLUSIONS

In this paper, two of the wavelet soft thresholding operators were modified in order to suit to the special characteristics of EMD modes. Moreover, an iterative scheme for improved EMD denoising performance was developed. The new algorithms, have been tested with two well studied signals in high to moderate noise scenarios and their performance was compared with wavelet thresholding methods. It turned out, that the iterative EMD denoising method outperforms the wavelet thresholding techniques in the cases that the signal SNR does not exceed 15 dB.

REFERENCES

[1] N. E. Huang et. al., "The empirical mode decomposition and the hilbert spectrum for nonlinear and non-stationary time series analysis," *Proc. R. Soc. Lond. A*, vol. 454, pp. 903–995, Mar. 1998.

[2] Y. Kopsinis and S. McLaughlin, "Investigation and performance enhancement of the empirical mode decomposition method based on a heuristic search optimization approach," *IEEE Trans. Signal Processing*, pp. 1–13, Jan. 2008.

[3] Y. Kopsinis and S. McLaughlin, "Improved emd using doubly-iterative sifting and high order spline interpolation," *Journal on Advances of Signal processing (JASP)*, vol. 2008, Article ID 128293, 8 pages, 2008. doi:10.1155/2008/128293.

[4] L. Cohen, *Time-Frequency Analysis*, Prentice Hall, 1995.

[5] S. Mallat, *A wavelet tour of signal processing*, Academic press, second edition, 1999.

[6] S. Theodoridis and K. Koutroumbas, *Pattern Recognition*, Academic press, third edition, 2006.

[7] A. Antoniadis and J Fan, "Regularization of wavelets approximations," *J. Am. Statist. Ass.*, vol. 96, pp. 939–967, 2001.

[8] P. Flandrin, G. Rilling, and P. Gonçalvès, *EMD equivalent filter banks, from interpetation to applications (in N. E. Huang and S. Shen, Hilbert-Huang Transform and Its Applications)*, World Scientific Publishing Company, first edition, 2005.

[9] N. E. Huang Z. Wu, *Statistical significance test of intrinsic mode functions, (in N. E. Huang and S. Shen, Hilbert-Huang Transform and Its Applications)*, World Scientific Publishing Company, first edition, 2005.

[10] A. O. Boudraa and J. C. Cexus, "Denoising via empirical mode decomposition," in *ISCCSP2006*, 2006.

[11] Y. Mao and P. Que, "Noise suppression and flaw detection of ultrasonic signals via empirical mode decomposition," *Russian Journal of Nondestructive Testing*, vol. 43, pp. 196–203, 2007.

[12] T. Jing-tian, Z. Qing, T. Yan, L. Bin, and Z. Xiao-kai, "Hilbert-huang transform for ECG de-noising," in *1st International Conference on Bioinformatics and Biomedical Engineering (ICBBE 2007)*, 2007.

[13] Y. Kopsinis and S. McLaughlin, "Empirical mode decomposition based denoising techniques," in *1st International Workshop on Cognitive Information Processing (CIP2008)*, 2008.